Construction and Building Materials 220 (2019) 214–227

Contents lists available at ScienceDirect

Construction and Building Materials

journal homepage: www.elsevier.com/locate/conbuildmat

# Preparation and anti-icing properties of a hydrophobic emulsified asphalt coating

Sen Han *, Tengfei Yao *, Xiaofei Yang

*Key Laboratory for Special Area Highway Engineering of Ministry of Education, Chang'an University, Xi'an City 710064, PR China*

## HIGHLIGHTS

- Hydrophobic anti-icing emulsified asphalt was prepared.
- The effect of hydrophobic agent roughness, dosage and incorporation method on hydrophobic effect was analyzed.
- Anti-icing and anti-skidding properties of hydrophobic coating were tested.
- An indoor simulated anti-icing test was designed and the evaluation criteria for anti-icing performance were proposed.
- The adhesion and durability between hydrophobic coating and asphalt pavement were improved by interfacial agent.

## ARTICLE INFO

*Article history:*
Received 26 March 2019
Received in revised form 2 June 2019
Accepted 3 June 2019
Available online 10 June 2019

*Keywords:*
Hydrophobic coating
Hydrophobic emulsified asphalt
Road surface anti-icing
Ice bonding strength

## ABSTRACT

Icing on asphalt pavement may lead to potential hazards for driving safety. To reduce the security risk, this paper aims at preparing a hydrophobic emulsified asphalt coating on asphalt pavement by adding a hydrophobic agent (HPA, Polytetrafluoroethylene powder) to emulsified asphalt. Considering the factors influencing hydrophobic effect, such as roughness of hydrophobic agent, dosage and incorporation method, the ice-repellency of hydrophobic emulsified asphalt coating was characterized by means of contact angle. It was found the hydrophobic properties of emulsified asphalt were significantly affected by roughness, dosage and incorporation methods of HPA and the highest contact angle was 94.3° when the HPA with 1250 meshes and dosage of 15% was added by the external addition method. Through the interlayer shear test and the indoor anti-icing test, hydrophobic asphalt pavement could reduce the bond strength between pavement and ice so that the ice layer could be easily broken and cleared, and the bond strength could be reduced by about 40% at 0.3 kg/m$^2$ dosage of hydrophobic emulsified asphalt. It was proved that the skid resistance performance of the hydrophobic emulsified asphalt coating could conform to the requirements of the specification. The addition of interfacial agent can significantly improve the adhesion between emulsified asphalt and aggregates. These findings demonstrated the potential of using hydrophobic emulsified asphalt coating on highways in adverse weather to provide better anti-icing performance and contribute to traffic safety in winter.



## 1. Introduction

After the rain and snow in winter, the accumulated water or snow on asphalt pavement is easy to freeze in the low-temperature environment, resulting in a sharp decline in the anti-skidding performance of the pavement [1]. On the pavement with ice and snow, the emergency braking distance is greatly increased which poses a serious threat to the safety of life and property of pedestrians and vehicles even causes serious traffic congestion inducing a series of traffic accidents [2]. In view of the icing problems on asphalt pavements, the frequently-used methods of removing ice currently include artificial mechanical snow removal, spraying chloride ice-melting agents, thermal melting technology include microwave heating, thermal cables, solar energy collection technology, and electrically conductive pavements [3–11]. Nevertheless, the methods above will either aggravate pollutants, corrode metal structures, reduce the performance of asphalt binders or be quite expensive.

A large number of literatures have shown that hydrophobic surfaces have good hydrophobic and anti-icing properties [12,13]. The larger contact angle and the smaller wetting lag angle can effectively make the droplets rolling and sliding on the surface of the object, thus making it difficult to freeze. Some researchers have also been devoted to investigate the preparation of super-hydrophobic

* Corresponding authors.
*E-mail addresses:* hyram_hs@chd.edu.cn (S. Han), 760229882@qq.com (T. Yao).

https://doi.org/10.1016/j.conbuildmat.2019.06.021
0950-0618/

materials with low cost, good hydrophobic effect and convenient construction [14–15]. Ammar et al. [16] studied the influence of nano-SiO2 on hydrophobicity and corrosion resistance of acrylic-silicone polymeric matrix. They discovered that coatings incorporated with 3 wt% nano-SiO2 exhibited the highest contact angle of 97.3° and significant improvements in corrosion resistance. Cao et al. [17] prepared a super-hydrophobic coating composed of acrylic polymer resin, silicone resin and nanoparticles. They found that this coating effectively retarded icing and the anti-icing property is related to the nanoparticle size. Meanwhile, many laboratory tests and field observations have been carried out to evaluate the deicing performance of super-hydrophobic pavement [18,19]. The results show that super-hydrophobic materials can effectively improve the anti-skid performance of pavement in climatic areas where severe weather (such as snow, frost and freezing rain) usually occurs [20]. Therefore, there is a potential of using hydrophobic materials in pavement surface layer for better anti-icing performance.

The contact angle is often used to quantify the wetting condition of a water droplet on a solid surface. The wetting state can be hydrophilic ($\theta > 90°$) or hydrophobic ($\theta < 90°$) [21]. The contact angle can be calculated using Young's equation [22] with the assumption that the solid surface is glazed, chemically homogeneous, and undissolved. However, When a droplet is placed on a rough surface, the real contact angle of the droplet on the solid surface can hardly be measured. The experimental results only show the apparent contact angle, but the apparent contact angle and the interfacial tension do not conform to Young's equation [23]. Wenzel and Cassie modified Young's equation from the thermodynamic point of view, and obtained Wenzel model and Cassie model. For the mode in Fig. 1a, water has completely infiltrated the rough grooves, which is called homogeneous wetting and can be described by the Wenzel model [24,25]. From the Fig. 1b, Cassie [26] believed that when the surface is more hydrophobic, the droplets cannot fill the cavity on the rough structure, and there would be trapped air under the liquid beads. Typically, surfaces described by the Wenzel model are sticky in that water droplets tend to adhere better than a flat counterpart, while those following the Cassie model are slippery in that water droplets tend to roll off more easily than a flat equivalent [27,28].

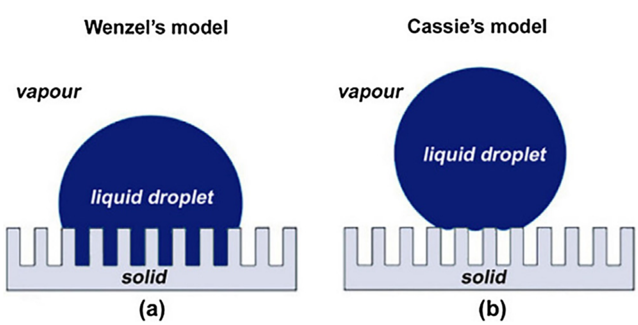


**Fig. 1.** Hydrophobic models: (a) Wenzel model; (b) Cassie model.

From Young's equation and Wenzel's theory, it can be concluded that preparation of materials with higher contact angles largely depends on constructing material surfaces with appropriate roughness densities to reduce the surface energies. A specific method is to construct a micro-/nano- structure on material surfaces with low surface energies [29]. On the basis of previous researches, this study focused on preparing a hydrophobic emulsified asphalt coating with hydrophobic and anti-icing properties, thus providing theoretical datum and technical support for the anti-icing at low temperature conditions in winter.

This study draws on the concept of the fog seal layer. A hydrophobic emulsified asphalt was prepared by adding a certain hydrophobic material (Polytetrafluoroethylene powder) to the emulsified asphalt. The hydrophobic agent (HPA) with good compatibility with emulsified asphalt was selected through experimental study, and the factors influencing hydrophobic effect, such as roughness of HPA, dosage and incorporation method, are studied and analyzed by means of contact angle test. After coating the specimens, the skid resistance performance was measured by British pendulum tester and sand patch method. Then the anti-icing performance of hydrophobic emulsified asphalt was observed by simulated icing test, simulation test of anti-icing and wettability test. Finally, the anti-icing performance of the hydrophobic emulsified asphalt coating was indirectly reflected by the measured adhesion data between the specimens and the ice layer. The flowchart of this research is shown in Fig. 2.

## 2. Materials and methods of experiment

### 2.1. Raw materials

- Asphalt: the matrix asphalt was SK90# with basic properties shown in Table 1.
- Emulsifier: cationic slow-cracking fast-setting emulsifier was used, and its properties are shown in Table 2.
- Hydrophobic agent (HPA): in this research, the Polytetrafluoroethylene (PTFE) powder was selected as the hydrophobic agent, which refers to a kind of substance having good hydrophobicity and hydrophobic migration. The HPA needs to be added in the emulsified asphalt with high speed mixer. In order not to damage the structure of the emulsified asphalt, and not to break the emulsion, the selected HPA must have stable molecular structure, excellent chemical resistance, aging resistance, UV resistance, scratch resistance, wide temperature range, and good hydrophobic properties even under low temperature condi-

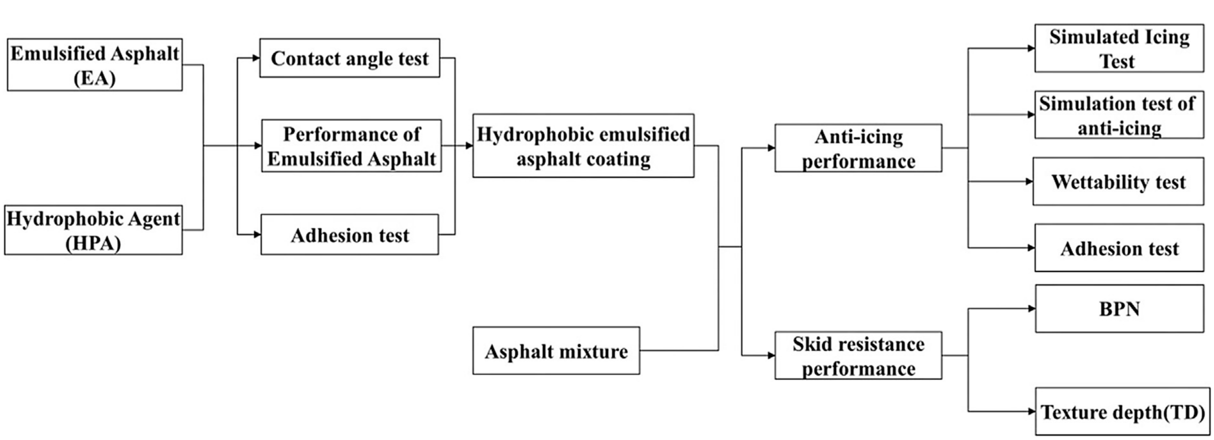


**Fig. 2.** The flowchart of this research.

**Table 1**
Properties of SK90# asphalt.

| Properties | | Results | Standard in China (JTG E20-2011) [30] |
|---|---|---|---|
| Penetration (25 °C, 100 g, 5 s)/0.1 mm | | 94 | T0604 |
| Softening point (Ring ball)/ °C | | 47.2 | T0606 |
| Ductility | (15 °C, 5 cm/min)/cm | >100 | T0605 |
| | (10 °C, 5 cm/min)/cm | >100 | T0605 |
| Dynamic viscosity (60 °C)/Pa·S | | 176 | T0625 |
| Flash point/ °C | | 287 | T0611 |
| Solubility/% | | 99.7 | T0607 |
| Wax content (Distillation)/% | | 1.4 | T0615 |

**Table 2**
Properties of emulsifier.

| Properties | Results |
|---|---|
| Active matter content | 65–70% |
| pH | 2.5–3.5 |
| State | Liquid |
| Dosage range | 1.5–2.0% |

tions. Three hydrophobic materials were selected in this paper, as shown in Fig. 3, which were mixed with emulsified asphalt and tested for comparison. According to the compatibility of the emulsified asphalt, the third HPA was selected, and its properties are shown in Table 3.

- Interfacial agent: the adhesion of emulsified asphalt to various aggregates is not as good as that of matrix asphalt which may not meet the requirements of specifications or barely meet the requirements. It is a mature technology to improve the adhesion between emulsified asphalt and aggregates by using silane interfacial agent [31]. The interface agent is an amino functional silane. Appearance of colorless or yellowish transparent liquid, versatile, soluble in organic solvents, soluble in water. The silane interfacial agent has both a group capable of bonding with an inorganic material and a group capable of bonding with an organic material. Its general formula can be represented by $Y(CH_2)_nSiX_3$. X represents a hydrolyzable methoxy group, an ethoxy group, a chlorine group, etc. These groups form silanol upon hydrolysis and then react with hydroxyl groups on the surface of the inorganic material to form hydrogen bonds and condense into -SiO-M- covalent bonds (M represents the surface of the inorganic material). Y represents an organic functional group such as an amino group or an epoxy group, and these groups are bonded by reaction with an organic substance [32]. Thereby the adhesion properties of the emulsified asphalt and the aggregate surface are improved. Its properties are shown in Table 4.
- PH regulator: in the production and preparation of emulsified asphalt, according to the different types of emulsifiers selected, the pH requirements of soap liquid would be different accordingly. In the process of preparing soap liquid, pH regulator was added according to actual needs to create a suitable environment for emulsifier to exert its activity, which could fully exert the effect of emulsifier, but also improving the storage stability of emulsified asphalt. Since the emulsifier selected in this study is cationic, the HCl solution is chosen as the pH regulator.

**Table 3**
Properties of HPA.

| Properties | Results |
|---|---|
| Appearance | White fine powder |
| Moisture content (%) | ≤0.03 |
| Tensile strength/(MPa) | 8 |
| Elongation at break | 60% |
| Apparent density (g/cm3) | 0.56 g/cm3 |
| Thermal weight loss (%Wt) | ≤0.2 |
| Corrosion resistance | Unchanged |
| Molecular weight | 10000–30000 |
| Melting point (°C) | 327 ± 5 |
| Decomposition temperature (°C) | 360 |
| Melt viscosity (Pa·S) | 102–106 |

### 2.2. Water droplet contact angle test

In this research, the hydrophobic properties of the pavement are indirectly characterized by the contact angle between the solid and liquid. 5 μL of water was dropped on a glass slide coated with hydrophobic emulsified asphalt by a syringe. The contact angle can be obtained by fitting with the software. The sessile drop and tangent line method were used to measure the contact angle by the contact angle detector [33], as shown in Fig. 4.

### 2.3. Preparation of hydrophobic emulsified asphalt

#### 2.3.1. Preparation of ordinary emulsified asphalt

In this study, the emulsified asphalt oil-water ratio is 5:5, the emulsifier content is 1.8%, and the selected colloid mill is RH-5 vertical colloid mill, as shown in Fig. 5 (a), (b). The rotational speed of colloidal mill is about 2870 r/min.

(1) Soap liquid preparation: heat the water (pH 6.0–8.5) that meets the requirements for use to 65–75 °C. According to the amount of emulsified asphalt to be prepared, the emulsifier and stabilizer are taken by scale, then water is slowly added and stirred to dissolve evenly. Continue to add water to the required mass of less than 5 g, then add the pH regulator to adjust to the required pH, and finally add water to the required quality with dropper.
(2) Asphalt heating: the asphalt is heated and melted in an oven at about 140C until it is in a state of melting with good fluidity.
(3) Preparation steps of emulsified asphalt.

a. Firstly, the colloid mill should be fully preheated. The proper amount of hot water is added into the colloid mill cycle to make the temperature of the colloid mill suitable to prevent the excessive temperature difference between the grinding body and soap liquor and asphalt from affecting the emulsification quality.
b. After fully preheating, drain hot water. The soap liquid with proper temperature is added into the colloid mill from the feed inlet, and the cycle is fully circulated until there is more foam.
c. The melted asphalt heated to the specified temperature is added slowly from the inlet, and should not be added at one time.
d. After being fully added, it was sheared in colloidal mill for 3–5 min, and observed whether there was segregation and agglomeration.
e. Open the valve, take out the prepared emulsified asphalt with a clean beaker, seal with plastic wrap and place it in an oven at 60° C for half an hour to defoam.

(a)HPA-1 (b) HPA-2 (c) HPA-3

**Fig. 3.** Macroscopic images of three different HPAs.

**Table 4**
Properties of Interfacial agent.

| Properties | Results |
|---|---|
| Boiling point/ °C | 217 |
| Density (ρ25 °C)/g/mL | 0.946 |
| Refractive index | 1.42 |
| Flash point/ °C | 104 |
| Molecular weight | 221.4 |
| Net contents | ≥97% |

According to the standard in China (JTG E20-2011) [30], in this study, evaporative residue content test, storage stability test, penetration, softening point, 10 °C ductility of evaporation residue, sieve residue test were carried out for the prepared emulsified asphalt. The data are shown in Table 5. The microstructure of emulsified asphalt was observed by fluorescence microscopy as shown in Fig. 6, and the storage stability of emulsified asphalt was further verified.

### 2.3.2. Preparation of hydrophobic emulsified asphalt

In order to explore the optimal hydrophobic performance and good road performance of hydrophobic emulsified asphalt, the factors including the roughness of HPA, the dosage of HPA and the incorporation method affecting the hydrophobic

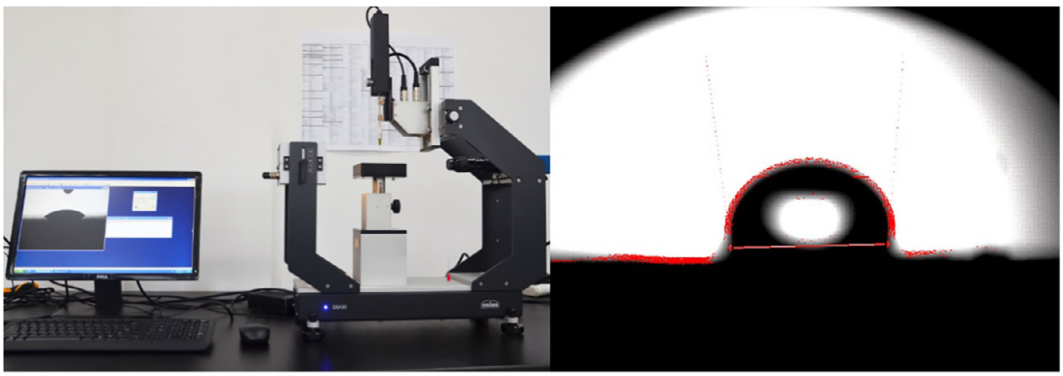

**Fig. 4.** Picture of contact angle detector and contact angle.

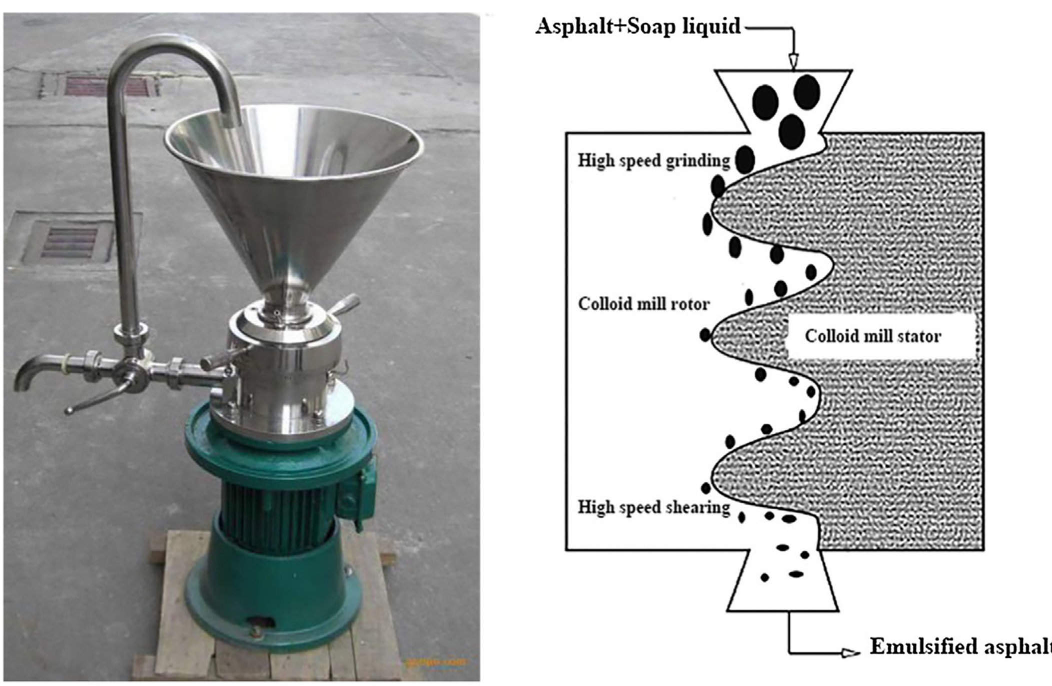


(a) (b)

**Fig. 5.** (a) The photo of Colloid mill; (b) Schematic diagram of emulsified asphalt production.

**Table 5**
Properties of emulsified asphalt.

| Properties | | Criteria | Results | Standard in China (JTG E20-2011) |
|---|---|---|---|---|
| Evaporative residue content/% | | >50 | 51.44 | T0651 |
| Storage stability (5d)/% | | ≤5 | 1.17 | T0655 |
| Evaporation residue | Penetration (25 °C, 100 g, 5 s)/0.1 mm | 50–200 | 72 | T0604 |
| | Softening point (Ring ball)/ °C | – | 51.7 | T0606 |
| | Ductility (10 °C, 5 cm/min)/cm | ≥40 | 70.2 | T0605 |
| Sieve residue/% | | ≤0.1 | 0.014 | T0652 |

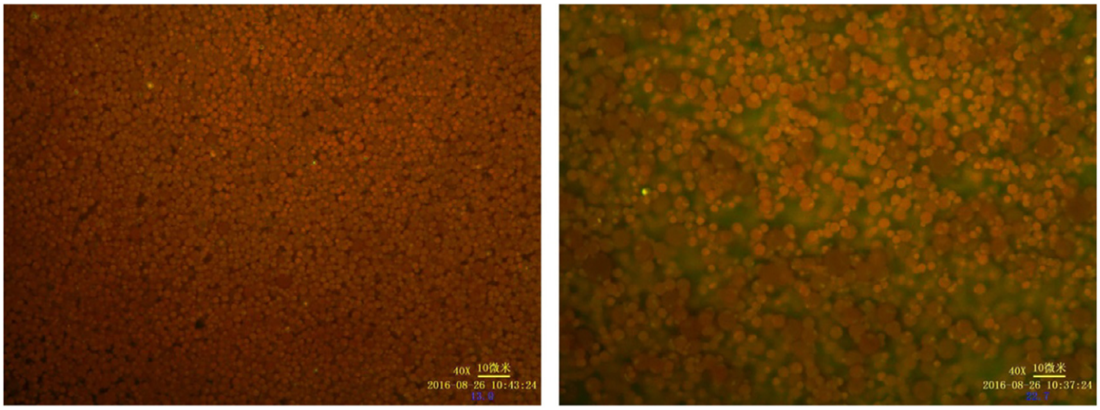

(a) (b)

**Fig. 6.** (a) Emulsified asphalt with good storage stability; (b) Emulsified asphalt with poor storage stability.

anti-icing performance of hydrophobic emulsified asphalt were considered. Moreover, the influence of HPA on asphalt performance and the adhesion between hydrophobic emulsified asphalt and different aggregates were also considered. Combined with the hydrophobic performance and pavement performance, the optimum proportion of hydrophobic emulsified asphalt was obtained.

The mesh number characterizes the roughness of the HPA. The larger mesh number, the greater the amount of HPA per unit area. In this research, HPA-3 in Fig. 1(c) was used. The mesh number are 625 (HPA-A), 800 (HPA-B), 1250 (HPA-C) and 2000 (HPA-D) in different roughness. Under the same dosage of emulsified asphalt (15%), they were uniformly sprayed on glass slide. After the demulsification was complete, the surface was washed with clean water, and the contact angle was measured by contact angle detector after drying. The change of the dosage of HPA and incorporation method would affect the hydrophobic properties of the emulsified asphalt. Therefore, 1250 meshes HPA was used to analyze the influence of different dosage on hydrophobic performance. The HPA dosage was 0%, 5%, 10%, 15%, 20%. The incorporation methods of HPAs were divided into internal addition method and external addition method. The operation flow is shown in Fig. 7.

Due to the incorporation of HPAs, the performance of the asphalt may be changed, affecting the various indexes of the asphalt, thereby affecting its pavement performance. In order to maximize the hydrophobic and anti-icing function of HPA, at the same time, ensure that asphalt indicators meet the requirements of specifications. In this study, 0%, 5%, 10%, 15% and 20% HPA were added into the matrix asphalt to test their penetration, softening point and 10 °C ductility respectively.

In order to verify that the hydrophobic emulsified asphalt added has sufficient adhesion between different aggregates. On the one hand, it is not easy to peel when it is directly sprayed; on the other hand, it is firmly bonded with aggregate when it is used as surface treatment, which can ensure that the hydrophobic characteristics of pavement can last as long as possible. Therefore, it is necessary to investigate its adhesion with different aggregates. The emulsified asphalt selected in this study is cationic. According to the specifications, the method of evaluating the adhesiveness of cationic emulsified asphalt is to observe that the wrapping area of crushed stone after water bath is larger than or less than 2/3. Referring to the evaluation criteria for the adhesion between asphalt and aggregate, we have prepared clearer and stricter evaluation criteria, as shown in Table 6.

In this study, representative alkaline limestone, neutral diabase and acid granite were selected as samples to evaluate the adhesion of emulsified asphalt to three different aggregates, and the adhesion grade was evaluated. The amount of interfacial agent was added evenly and slowly in the emulsified asphalt prepared in advance. The amount of the interface agent added was 0.0%, 0.3%, 0.6%, 0.9%, 1.2%, and 1.5%. Meanwhile, their adhesion with three kinds of stone was determined.

**Table 6**
Evaluation criteria and classification of hydrophobic emulsified asphalt adhesion.

| Peeling of Emulsified Asphalt Film | Adhesion grade |
|---|---|
| The emulsified asphalt film is completely preserved, and the surface of the aggregate is evenly covered with a black oil film. The asphalt film is peeled off slightly, and the percentage of falling area is less than 5. | V |
| The emulsified asphalt film is completely preserved, and some asphalt film is peeled off on the surface of the aggregate. The percentage of peeling area is between 5 and 20. | IV |
| The surface of the aggregate is unevenly covered with a yellow and black phase oil film. The percentage of peeling area is between 20 and 40. | III |
| The surface of the aggregate is unevenly covered with a black oil film, and there is a serious asphalt film shift. The peeling area percentage is between 40 and 60. | II |
| The asphalt film on the aggregate surface has a serious change, and the percentage of the peeling area is >60. | I |

*2.4. Pavement performance and anti-icing test of hydrophobic emulsified asphalt coating*

*2.4.1. Skid resistance test*

Following the ASTM E303-93 standard, the skid resistance was measured in wet condition. This difficulty was due to high water repellency of the surfaces, and the water droplets beaded up each time the wetting of the surfaces was attempted. In addition to measuring the BPN values in wet condition – which was in accordance with the ASTM E303-93 standard, Ali Arabzadeh et al. [34] decided to measure the BPN values in dry condition for the sake of comparison. Six 300 mm × 300 mm × 60 mm specimens were formed in the laboratory. The gradation of the specimens was commonly used in engineering application. The gradation is shown in Table 7. Firstly, The BPNs were measured on the uncoated samples at wet and dry conditions respectively. Then the prepared hydrophobic emulsified asphalt was evenly sprayed on the pre-prepared specimens according to 0.2 kg/m$^2$, 0.4 kg/m$^2$ and 0.6 kg/m$^2$ respectively, as shown in Fig. 8. The specimens were divided into three groups, and two specimens in each group were used

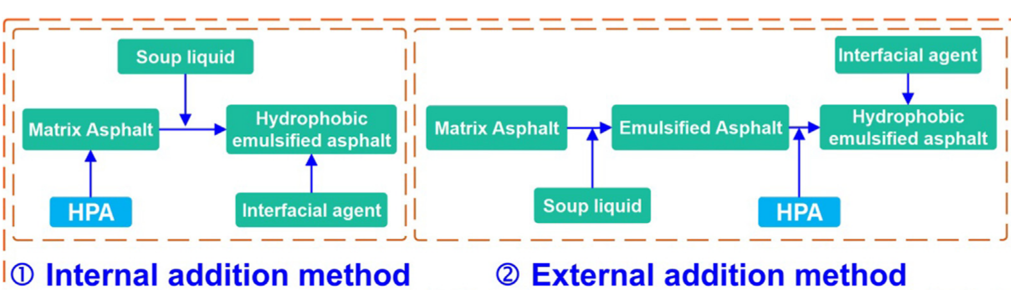


**Fig. 7.** The incorporation methods of HPAs.

**Table 7**
Gradation of asphalt mixture specimens.

| Sieve diameter (mm) | 16 | 13.2 | 9.5 | 4.75 | 2.36 | 1.18 | 0.6 | 0.3 | 0.15 | 0.075 | Mineral powder |
|---|---|---|---|---|---|---|---|---|---|---|---|
| Percentage through mass (%) | 100 | 94 | 81 | 70 | 88 | 89 | 96 | 96 | 98 | 94 | 94 |
| Percentage of sieve residue (%) | | 6 | 19 | 30 | 12 | 11 | 4 | 4 | 2 | 6 | 6 |

**Fig. 8.** Specimens Sprayed with Different Quantities of Hydrophobic Emulsified Asphalt.

as parallel test. The BPNs were measured on the coated samples at wet and dry conditions respectively. The texture depth (TD) of the pavement of specimens before and after spraying hydrophobic emulsified asphalt were measured by texture depth measurement referenced the Chinese standard of "Specifications for Design of Highway Asphalt Pavement" JTG D50-2017 [35]. The testing devices for measuring BPN and TD are shown in Fig. 9(a), (b), respectively.

*2.4.2. Simulated icing test of hydrophobic anti-icing coating*

The freezing time of droplets was observed on the hydrophobic and non-hydrophobic surfaces to study the freezing retardation of hydrophobic coatings, and the freezing time interval of droplets was calculated as the freezing delay time of surface. Two groups of specimens were prepared. One group of non-sprayed hydrophobic emulsified asphalt specimens served as control group. The other group of specimen was sprayed with hydrophobic emulsified asphalt. The two groups of specimens were put into the refrigerator at −10 to 5 °C. After 8 h of freezing, three droplets of water were dripped on the surface of each group of specimens with a plastic dropper, then continuous observation was made to record the solidification time of the droplets.

*2.4.3. Simulation test of anti-icing*

In this research, using the kinetic energy generated by the free falling of the ball from the height to impact the ice layer, the force of vehicle load on the ice layer on the actual road was simulated. The change of the adhesion between the ice layer and the road was characterized by observing the ice breakdown (crack, breakdown area, etc.). The schematic diagram and photo of simulation test of anti-icing are shown in Fig. 10. The test steps are as follows:

(1) The Marshall specimens were cut from the middle of the cross section as the specimens of simulation test of anti-icing.
(2) In this test, the experimental group and the control group were used. The control group was sprayed with ordinary emulsified asphalt on the cut specimens, and the experimental group was sprayed with hydrophobic emulsified asphalt.
(3) The prepared specimens were washed and dried with clean water, and then wrapped and sealed around the specimens with tape to form a bowl shape to prevent liquid loss.
(4) The specimens were frozen in the refrigerator with the temperature controlled from – 10 to −5 °C. When the temperature of the specimens dropped below zero, the same amount of water was added to the specimens and placed for 24 h to control the thickness of the ice layer to be substantially the same.
(5) Taking the specimens out of the refrigerator, taking out the tape wrapped around them, put the processed specimens into the refrigerator again, and taking out the specimens one by one for test. The process should be rapid, so as to prevent the high room temperature from affecting the test results.
(6) The specimens were placed on the base of the test device, and then the steel ball with diameter of 2.5 cm was freely dropped from the upper part of the device without initial velocity release. The anti-icing effect was analyzed by observing the ice breakage and crack of the specimens.

The destruction process of ice on the surface of the road is generally described as cracks, fracture and removal of the ice layer. In order to accurately evaluate the anti-icing performance of hydrophobic emulsified asphalt, the deicing effect was evaluated based on the research status of anti-icing by hydrophobic emulsified asphalt. The classification index for road deicing effect in this research is shown in Table 8.

*2.4.4. Wettability test*

Asphalt pavement is an organic whole formed by asphalt, aggregate, mineral powder and various additives. Therefore, the hydrophobic performance of the pavement is mainly determined by various components. For this reason, we sprayed the prepared hydrophobic emulsified asphalt on the asphalt concrete specimens for wettability test. Two groups of the same asphalt mixture sample plates were selected, one group was not treated as the control group, the other group was sprayed with a certain amount of hydrophobic emulsified asphalt as the experimental group. The same amount of water was sprayed on the surface of the two groups of specimens, and the movement of surface water flow was observed.

*2.4.5. Adhesion test*

The adhesion force between the ice layer and the pavement slab mainly refers to the size of the adhesion force between the ice layer and the pavement after the surface of the pavement is covered with ice. In this study, the shear test was used to characterize the adhesion between the ice layer and the asphalt mixture specimens. The hydrophobic emulsified asphalt containing different dosage of HPA was evenly spread on the specimens in advance at 0.3 kg/m$^2$. After the emulsion was completely broken, the surface was rinsed with clean water until no foam generated, and the ice was coated at −10 °C for shear test.

(a)

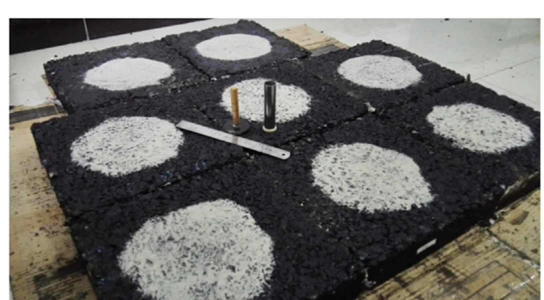

(b)

**Fig. 9.** The test devices for measuring BPN and TD: (a) Pendulum friction coefficient tester, (b) Test of texture depth.

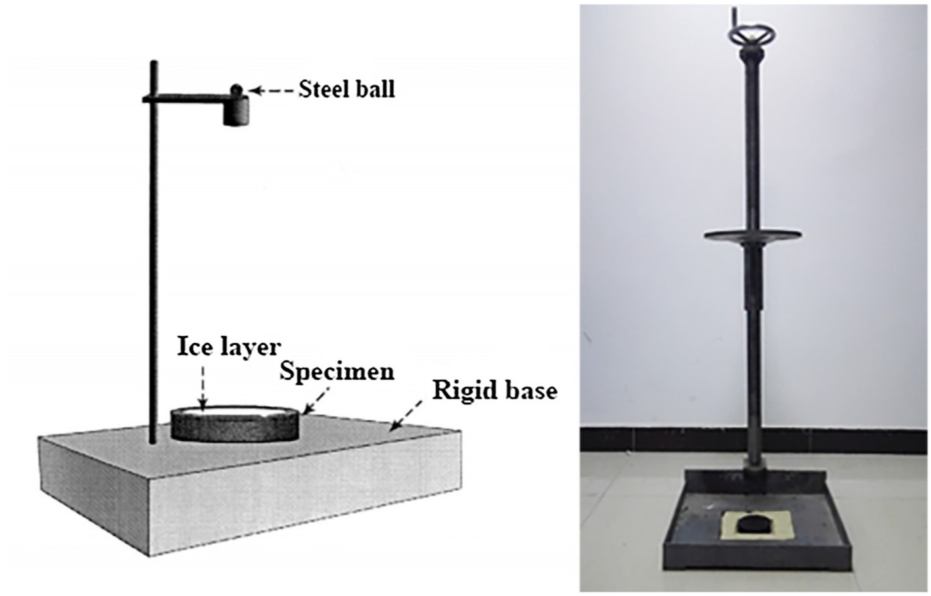


**Fig. 10.** The schematic diagram and photo of simulation test of anti-icing.

**Table 8**
Evaluation grade of pavement deicing effect.

| Grade | The state of ice destruction |
|---|---|
| I | Radial cracks occur in the ice layer. The rupture area is larger than the diameter of the steel ball, and part of the cracks are peeled off. |
| II | Radial cracks occur in the ice layer. The rupture area is larger than the diameter of the steel ball, and there is no obvious spalling. |
| III | There are few cracks and no radiation in the ice layer. The crack area is smaller than the diameter of the steel ball, and there is no obvious peeling off. |
| IV | There are no cracks in the ice layer, only impact pits and no peeling off. |

## 3. Results and discussion

### 3.1. Water droplet contact angle test

From Table 9, it can be seen that the hydrophobic effect increases with the increase of roughness under the same amount of HPA. The hydrophobic effect of HPA-C and HPA-D is better than that of HPA-A and HPA-B. The contact angle of emulsified asphalt with HPA-C and HPA-D is >90° which belongs to hydrophobic interface. The mesh number characterizes the roughness of the hydrophobic agent. The larger the mesh number, the finer the hydrophobic agent and the larger the specific surface area. The finer hydrophobic agent might be more easily dispersed uniformly into the emulsified asphalt. Meanwhile, another reason might be that the emulsified asphalt per unit area is exposed to a larger amount of hydrophobic agent. Thereby the finer hydrophobic agent can achieve a better hydrophobic effect. However, according to Fig. 11, when the mesh number of HPA is from 1250 mesh to 2000 mesh, the increasing trend of contact angle slowed down gradually. It might be due to some HPA particles will accumulate on the surface without binding to the substrate or HPA might not be evenly mixed with emulsified asphalt to cause the HPA particles deposition. the HPA was selected as 1250 meshes (HPA-C) with Comprehensive consideration of material cost and hydrophobic effect.

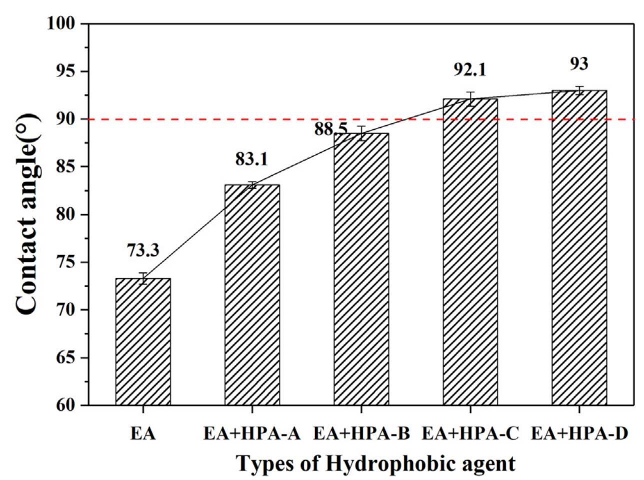


**Fig. 11.** Contact angle of emulsified asphalt mixed with different HPAs.

**Table 9**
Contact angle detection results of different roughness of hydrophobic agent.

| Test items | Contact angle (°) | | | | | | |
|---|---|---|---|---|---|---|---|
| | Test values | | | | Ave. | SD | CV |
| EA | 73.8 | 72.9 | 73.8 | 72.7 | 73.3 | 0.50 | 0.007 |
| EA+HPA-A | 82.8 | 82.8 | 83.2 | 83.5 | 83.1 | 0.29 | 0.004 |
| EA+HPA-B | 89.3 | 88.3 | 88.7 | 87.5 | 88.5 | 0.65 | 0.007 |
| EA+HPA-C | 92.5 | 91.7 | 92.9 | 91.3 | 92.1 | 0.63 | 0.007 |
| EA+HPA-D | 93.3 | 92.6 | 92.8 | 93.5 | 93.0 | 0.36 | 0.004 |

*Note*: EA = Emulsified asphalt, HPA = Hydrophobic agent, Ave. = Average, SD = Standard deviation, CV = Coefficient of variation.

**Table 10**
Contact angle detection results of different dosages of hydrophobic agent.

| Test items | Contact angle (°) | | | | | | |
|---|---|---|---|---|---|---|---|
| | Test values | | | | Ave. | SD | CV |
| EA | 73.8 | 72.9 | 73.8 | 72.7 | 73.3 | 0.50 | 0.007 |
| EA+5%HPA | 84.8 | 85.8 | 85.5 | 83.7 | 85.0 | 0.81 | 0.010 |
| EA+10%HPA | 86.4 | 87.7 | 87.7 | 87.5 | 87.3 | 0.54 | 0.006 |
| EA+15%HPA | 92.5 | 91.7 | 92.9 | 91.3 | 92.1 | 0.63 | 0.007 |
| EA+20%HPA | 94.3 | 93.6 | 92.9 | 93.6 | 93.6 | 0.49 | 0.005 |

*Note*: EA = Emulsified asphalt, HPA = Hydrophobic agent, Ave. = Average, SD = Standard deviation, CV = Coefficient of variation.

Table 10 shows the hydrophobic effect increases with the increasing amount of HPA when the HPA is the same. The hydrophobic effect of 15% and 20% is obviously better than that of 0%, 5% and 10%, and the contact angle is >90°, which belongs to the hydrophobic interface. However, according to Fig. 12, from HPA-C to HPA-D, the increasing trend of hydrophobic effect slowed down gradually. Considering the cost and economy, the optimum dosage of HPA was selected as 15%. From the comprehensive analysis of the above test results, it can be seen that the hydrophobic effect is constantly improving with the increasing number and content of HPAs. This may be due to the increasing effective components per unit area of HPA, which gradually forms a hydrophobic film on its surface, and gradually transits from non-hydrophobic interface to hydrophobic interface.

When the roughness and amount of HPA (15%) were determined, the influence of the way of HPA incorporation on hydrophobic effect was investigated. As is shown in Table 11, the hydrophobic effect of external addition method is better than that of internal addition method. The reason may be that the HPA added by the addition method does not react with the emulsified asphalt, and the density of the HPA is low. Under this addition method, it is not completely covered by asphalt and easy to dissociate with the surface, which is more conducive to its good hydrophobic performance.

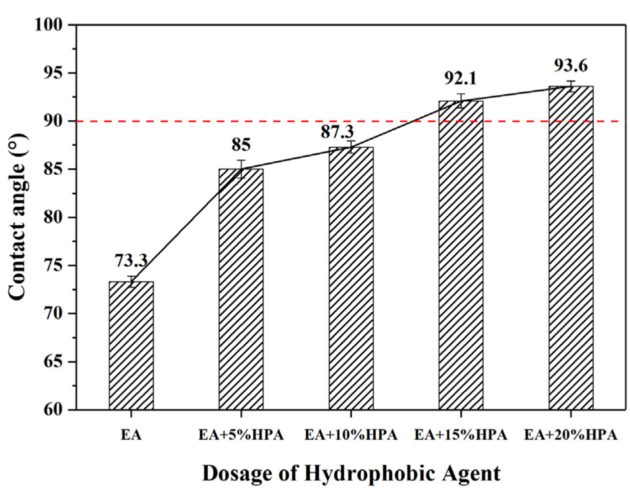


**Fig. 12.** Contact angle of hydrophobic emulsified asphalt with different dosage of HPA.

### 3.2. Influence of HPA dosage on asphalt performance

From Fig. 13, it can be seen that the softening point of asphalt increases slightly with the increase of HPA dosage, and the penetration of asphalt decreases obviously with the addition of HPA. However, with the increase of HPA dosage, the penetration decreases gradually and become flat, which still belongs to 90# asphalt. According to the Fig. 14, the 10 °C ductility decline is a bit more, but it still meets the specification requirements. When the doping amount increases to 20%, the ductility is close to the lower limit of the specification, so the maximum doping amount is 20%. This may be due to the fact that PTFE powder is insoluble in asphalt. It would be deposited during a period of time after high-speed mixing. Therefore, the inhomogeneity of hydrophobic emulsified asphalt could lead to the decrease of low temperature performance. In general, the participation of HPA will slightly affect the low-temperature performance of asphalt which fully meets the requirements of use.

### 3.3. Adhesion of hydrophobic emulsified asphalt to aggregate

From Table 12, when no interfacial agent was added, the adhesion rating of alkaline limestone and basic diabase to emulsified asphalt is both III, but it still needs to be improved. Acidic granite has relatively poor adhesion compared with the first two kinds of stone. With the increase of interfacial agent, the adhesion of

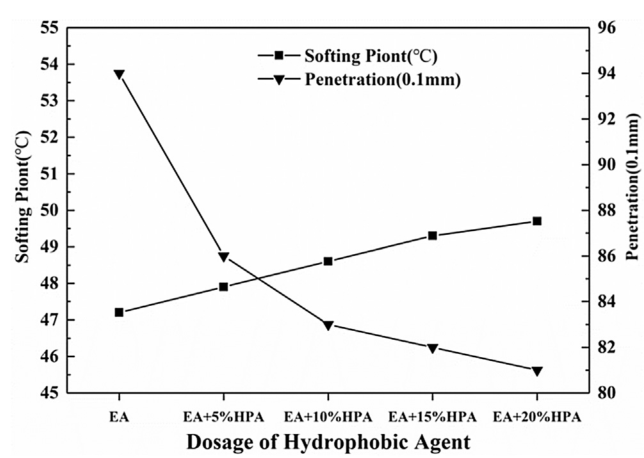


**Fig. 13.** Softening Point and Penetration of EA with different HPA Dosages.

**Table 11**
Contact angle test results of different incorporation methods.

| Incorporation method | Contact angle | | | | | |
|---|---|---|---|---|---|---|
| | Test results | | | | Mean | Standard error |
| Internal addition method | 92.2 | 91.2 | 92.1 | 91.3 | 91.7 | 0.23 |
| External addition method | 93.5 | 94.3 | 93.0 | 93.4 | 93.6 | 0.24 |

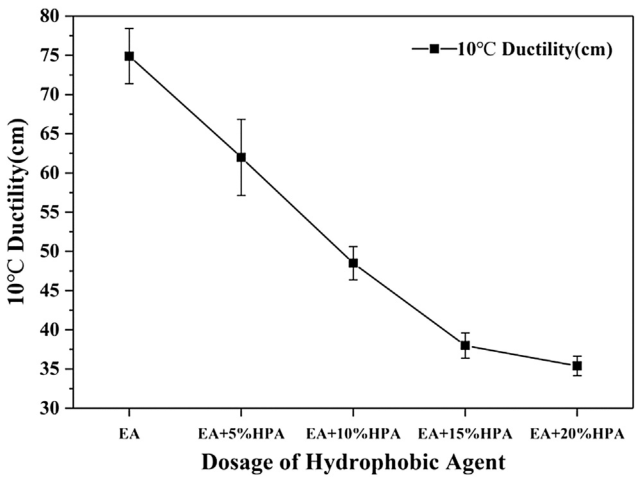


**Fig. 14.** 10 °C Ductility of EA with with different HPA Dosages.

emulsified asphalt and three kinds of aggregate with different properties was improved obviously.

The results of comprehensive analysis show that the recommended amount of interfacial agent is about 0.9%, which can improve the adhesion of emulsified asphalt to three different aggregates, and the adhesion of acid granite is also improved to grade IV–V. The interfacial agent can form bonds between asphalt and aggregate, HPA and aggregate so that make the connection between them more firm and enhance their durability. The improvement of adhesion can improve the durability of hydrophobic emulsified asphalt on the pavement. In addition, the interfacial agent can stabilize the HPA and make the hydrophobic performance of hydrophobic emulsified asphalt more durable. The improvement of the adhesion of interfacial agent to the granite with the worst adhesion is shown in Fig. 15.

### 3.4. Pavement performance and anti-icing test of hydrophobic emulsified asphalt coating

#### 3.4.1. Skid resistance test

From Tables 13 and 14, in both wet and dry conditions, When the surface of the specimen was sprayed with hydrophobic emulsified asphalt, the respective BPN values decreased to different extents. And as the amount of spray increased, its corresponding BPN value also decreased. In wet condition, when the spray amount was 0.6 kg/m$^2$, the measured BPN values on the wet uncoated specimens were 69.40 and 68.55 respectively. However, after measuring the skid resistance on the coated surface, the BPN value dropped approximately by 48%, resulting in the obtained values of 35.5 and 35.65 respectively. This behavior can be attributed to the spray amount of hydrophobic emulsified asphalt which was excessively sprayed caused the hydrophobic emulsified asphalt to cover the surface texture of the specimens. In dry condition, compared with the wet condition, the dry coated specimens caused a smaller drop in BPN, which was approximately 33%, and resulted in the obtained values of 57.40 and 57.45 respectively in the 0.6 kg/m$^2$ sprayed amount. According to "Technical Specifications for Maintenance of Highway Asphalt Pavement JTJ 073.2" [36], it is suggested that the amount of hydrophobic emulsified asphalt should not exceed 0.6 kg/m$^2$ to ensure that the anti-skid performance of pavement reaches a better state (see Fig. 16).

From Table 15, When the surface of the specimen was sprayed with hydrophobic emulsified asphalt, the respective TD values also decreased. When the spray amount was 0.6 kg/m$^2$, the measured TD values on the wet uncoated specimens were 0.84 and 0.86 respectively. However, after measuring the TD values on the coated surface, the TD values dropped approximately by 34%, resulting in the obtained values of 0.56 and 0.53 respectively. Meanwhile, the texture depth is close to the lower limit of the specification (see Fig. 17). In order to ensure the anti-skid performance and better hydrophobic and anti-icing performance, it is suggested that the spraying amount should be 0.2–0.4 kg/m$^2$.

**Table 12**
Adhesion test of emulsified asphalt to aggregate.

| Interface agent dosage | 0.0% | 0.3% | 0.6% | 0.9% | 1.2% | 1.5% |
|---|---|---|---|---|---|---|
| | Rating | | | | | |
| Limestone (alkaline) | III | IV | IV | V | V | V |
| Diabase (neutral) | III | III | IV | V | V | V |
| Granite (acid) | II | II | III | IV | V | V |


**Fig. 15.** Effect diagram before and after the improvement of adhesion between emulsified asphalt and granite.

**Table 13**
Measured BPN values in wet condition.

| The spray amount of HEA (kg/m$^2$) | Before coating | | After coating | | RSR |
|---|---|---|---|---|---|
| | Ave. | SE | Ave. | SE | % |
| 0.2 | 68.25 | 0.24 | 58.30 | 0.47 | 14.58 |
| | 67.50 | 0.17 | 56.75 | 0.55 | 15.93 |
| 0.4 | 64.75 | 0.28 | 46.25 | 0.63 | 28.57 |
| | 66.50 | 0.32 | 47.10 | 0.58 | 29.17 |
| 0.6 | 69.40 | 0.55 | 35.50 | 0.78 | 48.85 |
| | 68.55 | 0.48 | 35.65 | 0.85 | 47.99 |

*Note*: HEA = Hydrophobic emulsified asphalt, Ave. = Average, SE = Standard error and RSR = Reduction in skid Resistance.

**Table 14**
Measured BPN values in dry condition.

| The spray amount of HEA (kg/m$^2$) | Before coating | | After coating | | RSR |
|---|---|---|---|---|---|
| | Ave. | SE | Ave. | SE | % |
| 0.2 | 84.20 | 0.18 | 73.75 | 0.33 | 12.41 |
| | 83.50 | 0.17 | 72.30 | 0.42 | 13.41 |
| 0.4 | 81.45 | 0.22 | 62.85 | 0.65 | 22.84 |
| | 82.30 | 0.36 | 63.30 | 0.38 | 23.09 |
| 0.6 | 86.55 | 0.29 | 57.40 | 0.36 | 33.68 |
| | 85.75 | 0.34 | 57.25 | 0.43 | 33.24 |

*Note*: HEA = Hydrophobic emulsified asphalt, Ave. = Average, SE = Standard error and RSR = Reduction in skid resistance.

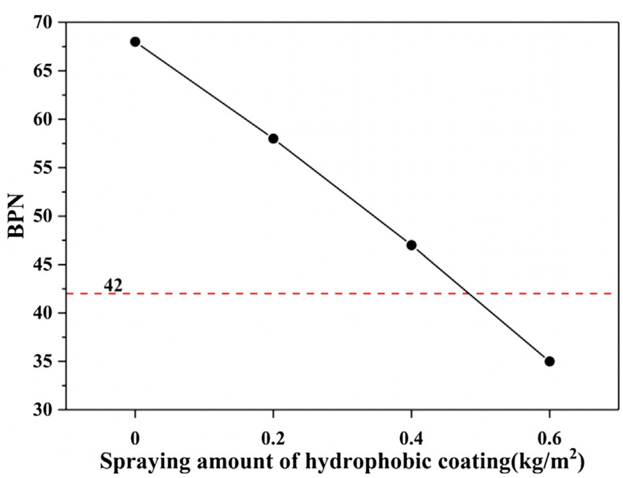


**Fig. 16.** BPN of hydrophobic coatings with different spraying amount in wet condition.

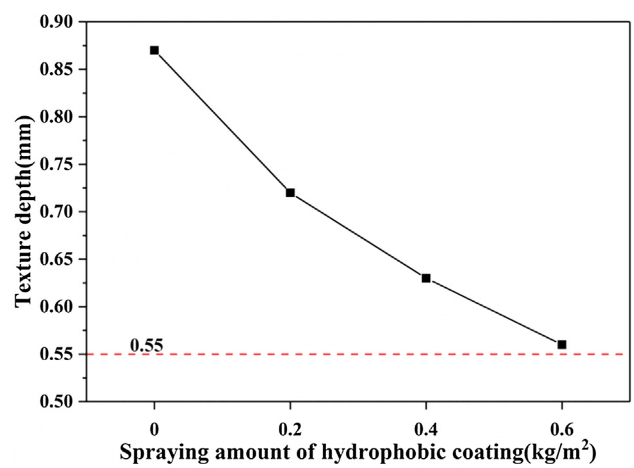


**Fig. 17.** Texture depth of hydrophobic coatings with different spraying amount.

There might be two possible reasons for the decline of pavement anti-skid performance. On the one hand, the existence of asphalt film might reduce the texture depth of road surface. On the other hand, the existence of asphalt film could cover part of the micro-structure of the road surface. However, with the road traffic opened, part of the asphalt film on the road surface is worn out, and the anti-skid performance of the road will be restored to a certain extent.

### *3.4.2. Simulated icing test of hydrophobic anti-icing coating*

During the 4–5th minute, the droplets in the control group had solidified into ice and the droplets in the experimental group began

**Table 15**
Measured texture depth values.

| The spray amount of HEA (kg/m$^2$) | Before coating | | After coating | | RSR |
|---|---|---|---|---|---|
| | Ave.(mm) | SE | Ave.(mm) | SE | % |
| 0.2 | 0.87 | 0.03 | 0.72 | 0.04 | 12.41 |
| | 0.83 | 0.02 | 0.70 | 0.02 | 13.41 |
| 0.4 | 0.82 | 0.02 | 0.63 | 0.05 | 22.84 |
| | 0.84 | 0.01 | 0.59 | 0.03 | 23.09 |
| 0.6 | 0.84 | 0.04 | 0.56 | 0.04 | 33.68 |
| | 0.86 | 0.03 | 0.53 | 0.02 | 33.24 |

*Note*: HEA = Hydrophobic emulsified asphalt, Ave. = Average, SE = Standard error and RSR = Reduction in skid resistance.

to solidify, so the delay time of freezing in the experimental group was judged between 4th and 5th minute. The Marshall specimens coated with hydrophobic coatings have better hydrophobic properties, which enlarges the barrier of the critical nucleus radius of the interface compared with the untreated interface, thus prolonging the formation of micro-ice crystals.

*3.4.3. Simulation test of anti-icing*

As shown in Fig. 18, during the test of common emulsified asphalt specimens, a small amount of cracks were produced in the ice layer under the action of ball loads, but no radial cracks were produced, no ice layer was obviously peeled off, and only the pits caused by the impact load of falling steel balls were found. After repeated tests at the same location, it was found that the ice layer did not change much, but the local pit formed by the deviation of the falling point of force. Based on the observation and analysis of the above experiments, the standard rating of the control evaluation was grade III.

Fig. 19 is the anti-icing test results of asphalt concrete specimens with hydrophobic coating. During the test, it was found that the ice layer produces radial cracks under the impact load of small steel balls, and the rupture area is obviously larger than the diameter of steel balls, accompanied by partial peeling and shedding. Under repeated tests at a single point, cracks gradually increase, interweave with each other and gradually exfoliate. Especially at the edge, under the action of small spherical loads, not only the radial cracks are obvious, but also the displacement is visible. Based on the above test results, the standard rating of the control evaluation was grade I.

**Table 16**
Evaluation results of simulation test of anti-icing of HPA with different HPA dosages.

| HPA dosage | 0% | 5% | 10% | 15% |
|---|---|---|---|---|
| Grade | III | II | I | I |

The hydrophobic emulsified asphalt with different dosage of HPA was tested separately. The experimental results are shown in Table 16. From the test results, it can be found that the ice layer of the samples sprayed with hydrophobic emulsified asphalt is fragile, flaky and accompanied by displacement under load, while the ice layer of the ordinary emulsified asphalt samples has no obvious change. Therefore, due to the role of hydrophobic emulsified asphalt, the adhesion force between the road surface ice and the road surface is significantly reduced, which makes the road surface ice easier to be broken and cleared, and makes the road surface hydrophobic and anti-icing.

*3.4.4. Wettability test*

As shown in Fig. 20, when water droplets are applied to specimens sprayed with hydrophobic emulsified asphalt, the water droplets have obvious shrinkage and aggregation phenomenon, while on specimens not sprayed with hydrophobic emulsified asphalt, the water droplets have no obvious shrinkage and aggregation

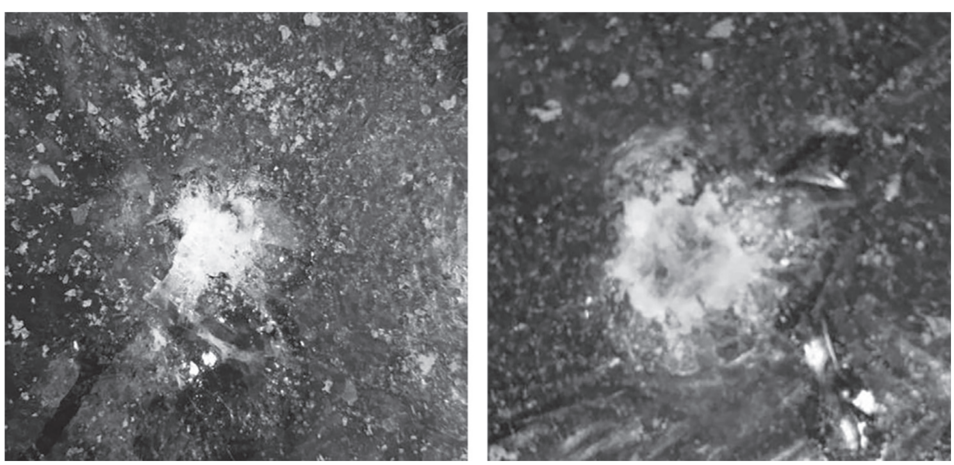

(a) Single action (b) Multiple action

**Fig. 18.** Simulation test of anti-icing of ordinary emulsified asphalt specimens.

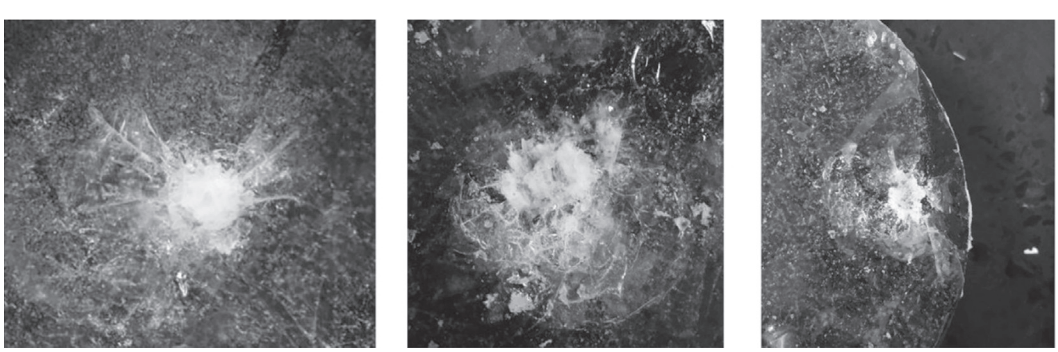

(a) Single action (b) Multiple action (c) Marginal single action

**Fig. 19.** Simulation test of anti-icing of Hydrophobic emulsified asphalt specimens.

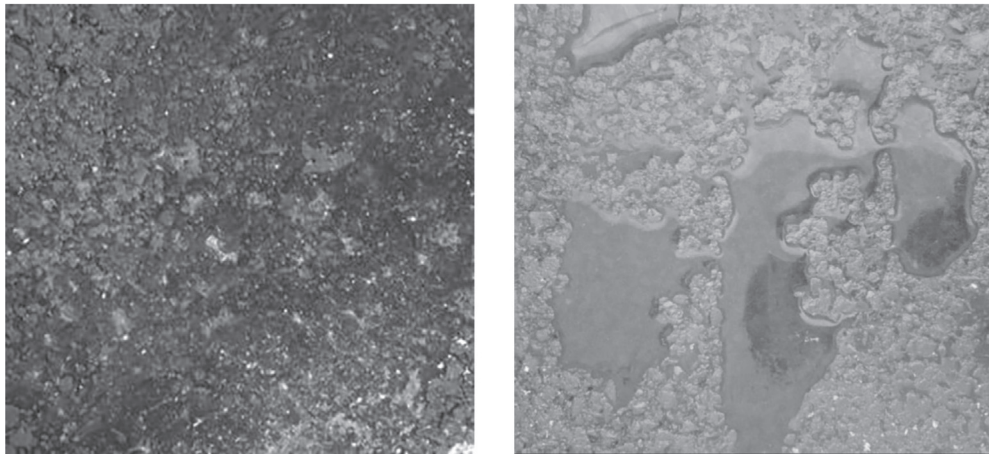

(a) Ordinary asphalt pavement (b) Hydrophobic anti-icing pavement

**Fig. 20.** Comparisons of wettability tests between ordinary asphalt pavement and hydrophobic anti-icing pavement.

**Table 17**
Adhesion force between ice layer and pavement.

| HPA dosage (%) | | | 0 | 5 | 10 | 15 |
|---|---|---|---|---|---|---|
| Internal addition method | Adhesion force (kN) | 1 | 1.494 | 1.392 | 1.092 | 1.182 |
| | | 2 | 1.818 | 1.206 | 1.2 | 1.17 |
| | | 3 | 1.572 | 1.452 | 1.17 | 1.08 |
| | mean (kN) | | 1.628 | 1.35 | 1.154 | 1.144 |
| | Standard Error | | 0.08 | 0.06 | 0.03 | 0.03 |
| | Decrease ratio of adhesion force (%) | | 0 | 17.08 | 29.12 | 29.73 |
| External addition method | Adhesion force (kN) | 1 | 1.494 | 1.266 | 1.05 | 0.978 |
| | | 2 | 1.818 | 1.362 | 1.134 | 0.804 |
| | | 3 | 1.572 | 1.248 | 0.984 | 1.11 |
| | mean (kN) | | 1.628 | 1.292 | 1.056 | 0.964 |
| | Standard Error | | 0.08 | 0.04 | 0.03 | 0.07 |
| | Decrease ratio of adhesion force (%) | | 0 | 20.64 | 35.14 | 40.79 |

phenomenon, and continue to diffuse. Before the freezing of ordinary asphalt pavement, ice water has penetrated into the interior of asphalt pavement, forming "ice whiskers" in the pore of asphalt pavement structure, tightly "pinning" the pavement, and the ice cover is uniform and continuous, covering the whole pavement, while the hydrophobic pavement will shrink and gather obviously because of the water droplets, the ice formed is discontinuous and distributed in local areas. The test shows that the hydrophobic emulsified asphalt can obviously improve the hydrophobic ice-proof performance of pavement.

*3.4.5. Adhesion test*

Table 17 shows the adhesion of ice layer and specimens under different addition methods and different HPA dosages. It could be found that the adhesion force between ice layer and specimens decreases gradually with the increase of HPA content. From Figs. 21 and 22, it is observed straightly that the effect of external addition method is better than that of internal addition method under the same dosage of HPA. When the dosage of HPA is 15%, the adhesion force of the external addition method decreases by about 40% compared with that of the non-hydrophobic coating. In contrast, the

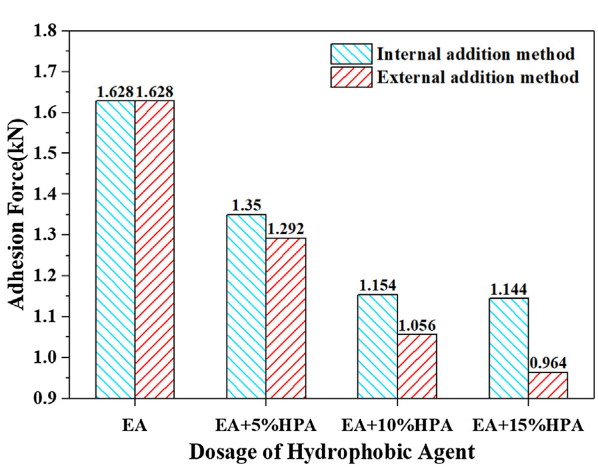


**Fig. 21.** Comparison of Adhesive Force of Different Addition Methods.

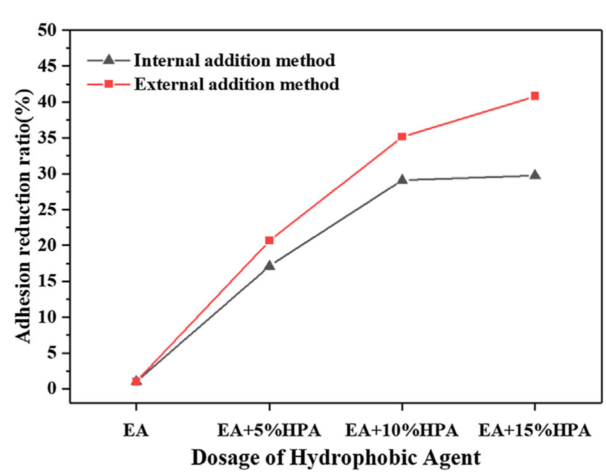


**Fig. 22.** Comparison of adhesion reduction ratios of different addition methods.

adhesion force of the internal addition method decreases by only about 30%. This may be due to the fact that the HPA doped by the internal addition method is completely encapsulated by asphalt, and the initial hydrophobic performance is not fully reflected.

## 4. Conclusion

In this work, a hydrophobic emulsified asphalt was formed by adding a hydrophobic material into the emulsified asphalt, then the pavement performance and anti-icing of the hydrophobic emulsified asphalt coating were tested. The major conclusions of this study drawn from the current test procedures are as follows:

(1) The hydrophobic properties of emulsified asphalt are significantly affected by roughness, dosage and incorporation methods of HPA. At the same amount of HPA, as its mesh number increases, the hydrophobic effect is continuously enhanced. At the same roughness of HPA, the hydrophobic effect increases with the increase of the dosage.
(2) The hydrophobic effect of external addition method is better than internal addition method. When the HPA with 1250 meshes and dosage of 15% is selected by the addition method, the highest contact angle is 94.3°.
(3) Hydrophobic emulsified asphalt coating can reduce the adhesion between ice and surface. On the surface of hydrophobic material, the formed ice could be removed under the action of vehicle load. When the dosage of HPA is 15%, the adhesion force of hydrophobic pavement decreases by about 40% compared with the original pavement.
(4) The interface agent has an obvious effect on improving the adhesion of the hydrophobic emulsified asphalt to the aggregate. When the interfacial agent dosage is about 0.9%, the adhesion of the emulsified asphalt to the three aggregates can be better improved.
(5) The hydrophobic coating could slightly reduce anti-skid performance of pavement. However, the anti-skid performance of the road can still meet the requirements under the appropriate amount of spraying, and the anti-skid coefficient will be restored in a period of time after the traffic is opened.

The conclusions obtained for this study demonstrate the potential of using hydrophobic emulsified asphalt coating on road surface in cold regions to provide better anti-icing and pavement performance and enhance traffic safety at winter seasons. This study has concentrated on hydrophobic and anti-icing performance and pavement performance of hydrophobic emulsified asphalt coating. Future research should be conducted to investigate mechanical performance and durability of hydrophobic emulsified asphalt coating. Field testing of hydrophobic emulsified asphalt coating is also needed to verify the finding obtained from laboratory experiments.

## Declaration of Competing Interest

None.

## Acknowledgements

This research was supported by National Natural Science Foundation of China (NSFC) (Grant No. 51578076) and the Fundamental Research Funds for the Central Universities, CHD (Grant No. 300102219207). These supports are gratefully acknowledged.

## References

[1] H.C. Dan, L.H. He, B. Xu, Experimental investigation on skid resistance of asphalt pavement under various slippery conditions, Int. J. Pavement Eng. 18 (2017) 485–499, https://doi.org/10.1080/10298436.2015.1095901.
[2] Konrad Jan Waluś. Driver's Strategy and Braking Distance in Winter. Proceedings of 21st International Scientific Conference. Transport Means. 2017.
[3] X. Shi, L. Fay, Z. Yang, A. Nguyen Tuan, Y. Liu, Corrosion of deicers to metals in transportation infrastructure: introduction and recent developments, Corros. Rev. (2009) 23.
[4] A. Galuszka, Z.M. Migaszewski, R. Podlaski, S. Dolegowska, A. Michalik, The influence of chloride deicers on mineral nutrition and the health status of roadside trees in the city of Kielce, Poland, Environ. Monit. Assess. 176 (2011) 451–464, https://doi.org/10.1007/s10661-010-1596-z.
[5] Z. Wang, T. Zhang, M. Shao, T. Ai, P. Zhao, Investigation on snow-melting performance of asphalt mixtures incorporating with salt-storage aggregates, Constr. Build. Mater. 142 (2017) 187–198, https://doi.org/10.1016/j.conbuildmat.2017.03.070.
[6] M. Chen, S. Wu, H. Wang, J. Zhang, Study of ice and snow melting process on conductive asphalt solar collector, Sol. Energy Mater. Sol. Cells 95 (2011) 3241–3250, https://doi.org/10.1016/j.solmat.2011.07.013.
[7] X. Liu, S.J. Rees, J.D. Spitler, Modeling snow melting on heated pavement surfaces. Part I: model development, Appl. Therm. Eng. 27 (2007) 1115–1124, https://doi.org/10.1016/j.applthermaleng.2006.06.017.
[8] X.W. Tang, S.J. Jiao, Z.Y. Gao, X.L. Xu, Study of 5.8 GHz magnetron in microwave deicing, J. Electromagn. Waves Appl. 22 (2008) 1351–1360, https://doi.org/10.1163/156939308786348901.
[9] X.-M. Zhou, Z.J. Yang, C. Chang, G. Song, Numerical assessment of electric roadway deicing system utilizing emerging carbon nanofiber paper, J. Cold Reg. Eng. 26 (2012) 1–15, https://doi.org/10.1061/(ASCE)CR.1943-5495.0000033.
[10] J.W. Daniels, E. Heymsfield, M. Kuss, Hydronic heated pavement system performance using a solar water heating system with heat pipe evacuated tube solar collectors, Sol. Energy 179 (2019) 343–351, https://doi.org/10.1016/j.solener.2019.01.006.
[11] Z. Hou, Z. Li, Z. Tang, Study on electrical properties of carbon fiber electrically conductive concrete for deicing or snowmelting, J. Wuhan Univ. Technol. 24 (8) (2002) 32–34.
[12] I. Izarra, J. Cubillo, A. Serrano, J.F. Rodriguez, M. Carmona, A hydrophobic release agent containing SiO2-CH3 submicron-sized particles for waterproofing mortar structures, Constr. Build. Mater. 199 (2019) 30–39, https://doi.org/10.1016/j.conbuildmat.2018.12.018.
[13] M. Zakerzadeh, S.M. Abtahi, A. Allafchian, M.R. Chamani, Examining the effect of different super hydrophobic nanomaterials on asphalt pavements, Constr. Build. Mater. 180 (2018) 285–290.
[14] G. Li, J. Yue, C. Guo, Y. Ji, Influences of modified nanoparticles on hydrophobicity of concrete with organic film coating, Constr. Build. Mater. 169 (2018) 1–7, https://doi.org/10.1016/j.conbuildmat.2018.02.191.
[15] W. She, X. Wang, C. Miao, Q. Zhang, Y. Zhang, J. Yang, J. Hong, Biomimetic superhydrophobic surface of concrete: topographic and chemical modification assembly by direct spray, Constr. Build. Mater. 181 (2018) 347–357, https://doi.org/10.1016/j.conbuildmat.2018.06.063.
[16] S. Ammar, K. Ramesh, B. Vengadaesvaran, S. Ramesh, A.K. Arof, A novel coating material that uses nano-sized SiO2 particles to intensify hydrophobicity and corrosion protection properties, Electrochim. Acta 220 (2016) 417–426, https://doi.org/10.1016/j.electacta.2016.10.099.
[17] L. Cao, A.K. Jones, V.K. Sikka, J. Wu, D. Gao, Anti-icing superhydrophobic coatings, Langmuir 25 (2009) 12444–12448, https://doi.org/10.1021/la902882b.
[18] C. Peng, H. Zhang, Z. You, F. Xu, G. Jiang, S. Lv, R. Zhang, H. Yang, Preparation and anti-icing properties of a superhydrophobic silicone coating on asphalt mixture, Constr. Build. Mater. 189 (2018) 227–235, https://doi.org/10.1016/j.conbuildmat.2018.08.211.
[19] Y. Gao, L. Qu, B. He, K. Dai, Z. Fang, R. Zhu, Study on effectiveness of anti-icing and deicing performance of super-hydrophobic asphalt concrete, Constr. Build. Mater. 191 (2018) 270–280, https://doi.org/10.1016/j.conbuildmat.2018.10.009.
[20] M. Zakerzadeh, S.M. Abtahi, A. Allafchian, M.R. Chamani, Examining the effect of different super hydrophobic nanomaterials on asphalt pavements, Constr. Build. Mater. 180 (2018) 285–290, https://doi.org/10.1016/j.conbuildmat.2018.04.190.
[21] Y. Lin, J. He, Recent progress in antireflection and self-cleaning technology – from surface engineering to functional surfaces, Prog. Mater. Sci. 61 (8) (2014) 94–143, https://doi.org/10.1016/j.pmatsci.2013.12.003.
[22] T. Young III, An essay on the cohesion of fluids, Philos. Trans. R. Soc. Lond. 95 (1805) 65–87, https://doi.org/10.1098/rstl.1805.0005.
[23] G. Whyman, E. Bormashenko, T. Stein, The rigorous derivation of young, cassie-baxter and wenzel equations and the analysis of the contact angle hysteresis phenomenon, Chem. Phys. Lett. 450 (2008) 355–359, https://doi.org/10.1016/j.cplett.2007.11.033.
[24] R.N. Wenzel, Resistance of solid surfaces to wetting by water, Ind. Eng. Chem. 28 (1936) 988–994, https://doi.org/10.1021/ie50320a024.

[25] A. Marmur, Super-hydrophobicity fundamentals: implications to biofouling prevention, Biofouling 22 (2006) 107–115, https://doi.org/10.1080/08927010600562328.
[26] A.B.D. Cassie, S. Baxter, Wettability of porous surfaces, Trans. Faraday Soc. 40 (1944) 546–551, https://doi.org/10.1039/TF9444000546.
[27] A. Marmur, The Lotus effect: superhydrophobicity and metastability, Langmuir 20 (2004) 3517–3519, https://doi.org/10.1021/la036369u.
[28] X. Zhang, L. Wang, E. Levänen, Superhydrophobic surfaces for the reduction of bacterial adhesion, RSC Adv. 3 (30) (2013) 12003–12020, https://doi.org/10.1039/c3ra40497h.
[29] C. Peng, P. Chen, Z. You, S. Lv, F. Xu, W. Zhang, H. Zhang, The anti-icing and mechanical properties of a superhydrophobic coating on asphalt pavement, Constr. Build. Mater. 190 (2018) 83–94, https://doi.org/10.1016/j.conbuildmat.2018.09.128.
[30] Standard Test Methods of Bitumen and Bituminous Mixtures For Highway Engineering JTJ E20-2011, China Communications Press, Beijing, 2011 (in Chinese).
[31] M. Xanthos, Interfacial agents for multiphase polymer systems: recent advances, Polym. Eng. Sci. 28 (1988) 1392–1400, https://doi.org/10.1002/pen.760282108.
[32] E.P. Plueddemann, Adhesion through silane coupling agents, J. Adhes. 2 (3) (1970) 184–201, https://doi.org/10.1080/0021846708544592.
[33] X. Zhang, F. Shi, J. Niu, Y. Jiang, Z. Wang, Superhydrophobic surfaces: from structural control to functional application, J. Mater. Chem. 18 (6) (2008) 621–633, https://doi.org/10.1039/b711226b.
[34] A. Arabzadeh, H. Ceylan, S. Kim, K. Gopalakrishnan, A. Sassani, S. Sundararajan, P.C. Taylor, Superhydrophobic coatings on Portland cement concrete surfaces, Constr. Build. Mater. 141 (2017) 393–401, https://doi.org/10.1016/j.conbuildmat.2017.03.012.
[35] Specifications for Design of Highway Asphalt Pavement JTG D50-2017, China Communications Press, Beijing, 2017 (in Chinese).
[36] Technical Specifications for Maintenance of Highway Asphalt Pavement JTJ 073-2001.2, China Communications Press, Beijing, 2001 (in Chinese).